Research Article

Ginsenoside Ro, an oleanolic saponin of *Panax ginseng*, exerts anti-inflammatory effect by direct inhibiting toll like receptor 4 signaling pathway

Hong-Lin Xu [a], Guang-Hong Chen [a], Yu-Ting Wu [a], Ling-Peng Xie [a], Zhang-Bin Tan [a, b], Bin Liu [a, b], Hui-Jie Fan [a, c], Hong-Mei Chen [a], Gui-Qiong Huang [d], Min Liu [e, **], Ying-Chun Zhou [a, *]

[a] School of Traditional Chinese Medicine, Department of Traditional Chinese Medicine, Nanfang Hospital (ZengCheng Branch), Southern Medical University, Guangzhou, China
[b] Department of Traditional Chinese Medicine, The Second Affiliated Hospital of Guangzhou Medical University, Guangzhou, China
[c] Department of Traditional Chinese Medicine, The First Hospital of Yangjiang, Yangjiang, China
[d] Department of Internal Medicine, Huizhou Hospital of Guangzhou University of Traditional Chinese Medicine, Huizhou, China
[e] Department of Pathogen Biology, Guangdong Provincial Key Laboratory of Tropical Disease Research, School of Public Health, Southern Medical University, Guangzhou, China

ARTICLE INFO

ABSTRACT

Background: Panax ginseng Meyer (*P. ginseng*), a herb distributed in Korea, China and Japan, exerts benefits on diverse inflammatory conditions. However, the underlying mechanism and active ingredients remains largely unclear. Herein, we aimed to explore the active ingredients of *P. ginseng* against inflammation and elucidate underlying mechanisms.
Methods: Inflammation model was constructed by lipopolysaccharide (LPS) in C57BL/6 mice and RAW264.7 macrophages. Molecular docking, molecular dynamics, surface plasmon resonance imaging (SPRi) and immunofluorescence were utilized to predict active component.
Results: P. ginseng significantly inhibited LPS-induced lung injury and the expression of pro-inflammatory factors, including TNF-α, IL-6 and IL-1β. Additionally, *P. ginseng* blocked fluorescence-labeled LPS (LPS488) binding to the membranes of RAW264.7 macrophages, the phosphorylation of nuclear factor-κB (NF-κB) and mitogen-activated protein kinases (MAPKs). Furthermore, molecular docking demonstrated that ginsenoside Ro (GRo) docked into the LPS binding site of toll like receptor 4 (TLR4)/myeloid differentiation factor 2 (MD2) complex. Molecular dynamic simulations showed that the MD2-GRo binding conformation was stable. SPRi demonstrated an excellent interaction between TLR4/MD2 complex and GRo (K_D value of 1.16×10^{-9} M). GRo significantly inhibited LPS488 binding to cell membranes. Further studies showed that GRo markedly suppressed LPS-triggered lung injury, the transcription and secretion levels of TNF-α, IL-6 and IL-1β. Moreover, the phosphorylation of NF-κB and MAPKs as well as the p65 subunit nuclear translocation were inhibited by GRo dose-dependently.
Conclusion: Our results suggest that GRo exerts anti-inflammation actions by direct inhibition of TLR4 signaling pathway.

1. Introduction

Inflammation is an innate immunity involving in many pathological progressions, protecting from external pathogens infections and cellular damage [1–3]. Macrophages, a major type of immune cells activated during inflammation, are able to synthesize and release pro-inflammatory cytokines, including interleukin (IL)-6, IL-1β and tumor necrosis factor (TNF)-α [4]. Systematic

* Corresponding author. School of Traditional Chinese Medicine, Southern Medical University, 1063 Shatai Road, Guangzhou, 510515, China.
** Corresponding author. School of Public Health, Southern Medical University, 1063 Shatai Road, Guangzhou, 510515, China.
E-mail addresses: ichbinlm@163.com (M. Liu), zhychun@126.com (Y.-C. Zhou).

inflammation has been previously revealed to increase the risk of autoimmune disorder, cardiovascular disease, neurodegenerative disorder, central insulin resistance, and cancer [5–9]. Therefore, modulating pro-inflammatory cytokines expression helps treat inflammatory diseases and might become a valid therapeutic strategy.

Acute lung injury (ALI) and its severer status, acute respiratory distress syndrome (ARDS), are common lung disorders in critical patients with a long hospitalization, which are characterized by excessive inflammation and structural destruction of lung tissue, with a fatality rate as high as 30% to 60% [10,11]. And it is pressing to exploit novel therapeutic strategies for ALI management. Moreover, mounting evidence has indicated the critical role of uncontrolled inflammation on the pathogenesis and development of ALI [12]. Therefore, suppressing an excessive inflammatory reaction might shed novel lights on ALI treatment.

Toll like receptor 4 (TLR4) plays a crucial role in the initiation of innate immunity [13,14]. Research reveals that TLR4 forms a heterodimer with its co-receptor, myeloid differentiation factor 2 (MD2) on the cell surface for identification, and signal initiation of lipopolysaccharide (LPS) [15]. Once LPS combining with MD2, TLR4-MD2 complex forms dimerization and subsequently activates nuclear factor-κB (NF-κB) and mitogen-activated protein kinases (MAPKs) signaling pathways, resulting in expression of the inflammatory factors [16]. Over-stimulation of this pathway causes serious inflammatory responses, further causing ALI and ARDS. Thus, it is of great significance to identify natural drugs that inhibit TLR4 activation to treat inflammation.

Panax ginseng Meyer (*P. ginseng*) as a traditional perennial plant has been widely used in Korea, Japan, and China. Accordingly, *P. ginseng* has been previously demonstrated to exhibit pharmacological actions in relieving symptoms of diverse diseases, such as inflammatory and autoimmune disorders, cardiovascular disorders, and cancer [17–20], most of which are involved in their pathological processes via systemic inflammations. Thus *P. ginseng* mediates inflammatory protection for these diseases. Moreover, *P. ginseng*, a single component or the component in complex prescriptions, is widely adopted in diverse antitussive remedies in Korea [21]. However, it remains largely unclarified of the underlying mechanism and the active ingredients of *P. ginseng* against inflammation. Therefore, herein, we aimed to explore the mechanism and active components of *P. ginseng*. Moreover, this research may offer other orientations of anti-inflammatory adjuvant for diverse inflammation-associated diseases.

2. Materials and methods

2.1. Materials

P. ginseng and ginsenoside Ro (GRo) with over 98% purity were purchased from Chengdu Must Biotechnology (Chengdu, China). Recombinant Human TLR4/MD2 Complex Protein was obtained from R&D Systems (Minneapolis, MN, USA). Antibodies targeting phospho-IκBα, phospho-p65, p65, phospho-JNK, JNK, phospho-P38, P38, phospho-ERK, ERK, and GAPDH were obtained from Cell Signaling Technology (Beverly, MA, USA). Antibodies targeting TLR4 was obtained from Zen Bioscience Co. Ltd (Chengdu, China). LPS (Escherichia coli O55:B5), fluorescence-labeled LPS (LPS488), Dexamethasone (DEX), and TLR4 selective inhibitor resatorvid

(TAK242) were from Sigma Aldrich (St. Louis, MO, USA). Other reagents were also commercially acquired.

2.2. Animal experiments

Six-weeks-old male C57BL/6 mice (18-22g) were obtained from the Animal Department (Southern Medical University, Guangzhou, China). The animal experimental procedures gained approval from Ethics Council of Southern Medical University (No. L2019147). Moreover, mice were fed with normal forage and accessible water in the humid environment of diurnal light-dark. ALI model was constructed according to the previous description [22]. Briefly, mice were assigned randomly into 9 groups (n = 10): control, LPS, LPS + *P. ginseng* low dose (50 mg/kg), LPS + *P. ginseng* middle dose (100 mg/kg), LPS + *P. ginseng* high dose (200 mg/kg), LPS + GRo low dose (20 mg/kg), LPS + GRo middle dose (40 mg/kg), LPS + GRo high dose (80 mg/kg) and LPS + DEX (5 mg/kg) groups. The test compounds dissolved with 3% tween-80 were orally administered to mice (200 μl/20 g) for consecutive five days, and the same amount of vehicle was administered to mice in the control and LPS groups, followed by intraperitoneal injection with LPS (10 mg/kg). All animals were euthanized 12 h after LPS-injection.

For toxicity evaluation of *P. ginseng* and GRo in animal model, an acute toxicity experiment was performed. Mice were assigned randomly into control, *P. ginseng* (orally received 50, 100, 200 mg/kg dose), and GRo groups (orally received 20, 40, 80 mg/kg dose). After oral administration for one week, The serum aspartate aminotransferase (AST) and alanine aminotransferase (ALT) were measured using commercial kits based on directions (Beyotime, Shanghai, China).

2.3. RAW264.7 cells cultivation and cell viability

RAW264.7 cells were cultured in DMEM supplemented with 10% FBS and 100 μg/ml penicillin and 100 μg/ml streptomycin at 37°C in a humidified atmosphere with 5% CO_2. MTT assay was adopted to examine cell viability according to the previous report [23].

2.4. Histopathological assessment of lung tissue

The lung tissue with 4% paraformaldehyde-immobilized and paraffin-embedded was cut into 4 μm slices and then stained by Haematoxylin and Eosin (H&E). The pathological modification was examined using the optical microscope (Nikon Eclipse Ti–S, Tokyo, Japan), and the lung injury score was evaluated by two pathologists as described previously [24].

2.5. Quantitative reverse transcription polymerase chain reaction (qRT-PCR)

RAW264.7 cells were seeded in 6-well plates and pretreated with gradient doses of *P. ginseng* or GRo for 24 h, then co-incubated with LPS (0.1 μg/ml) for 6 h. Trizol reagent (TaKaRa, Dalian, China) was used for total RNA isolation, followed by cDNA synthesis based on manufacturer's directions. PCR re-action was performed by SYBR Green I™ Premix Ex Taq PT™ kits (RR420A, TaKaRa) by StepOne plus PCR system (Waltham, MA, USA) according to the previous description [25]. The primers were as follows: TNF-α: forward 5′-TGGAACTGGCAGAAGAGGCAC-3′ and reverse 5′-

AGGGTCTGGGCCATAGAACTGA-3′. IL-6: forward 5′-TAGTCCTTCC-TACCCCAATTTCC-3′ and reverse 5′-TTGGTCCTTAGCCACTCCTTC-3′. IL-1β: forward 5′-TTCAGGCAGGCAGTATCACTC-3′ and reverse 5′-GAAGGTCCACGGGAAAGACAC-3′. GAPDH: forward 5′-AGGTCGGTGTGAACGGATTTG-3′ and reverse 5′-TGTA-GACCATGTAGTTGAGGTCA-3′. The lung tissue was homogenized by an impeller and then performed as mentioned above. GAPDH was utilized to normalize target genes and data quantification was performed using $2^{-\Delta\Delta Ct}$ method.

2.6. TNF-α, IL-6 and IL-1β secretion

Mouse enzyme-linked immunosorbent assay (ELISA) reagents (Dakewe, Shenzhen, China) were employed to explore the impacts of test compounds on TNF-α, IL-6, and IL-1β production. After treatment, the secretion of these pro-inflammatory cytokines were measured based on the directions.

2.7. Western blotting

Briefly, protein samples were dissolved with RIPA buffer and the concentrations were assessed by a BCA Protein Assay Kit (Beyotime). Then, 30 μg proteins were separated on 10% SDS-PAGE, and then transferred to PVDF membrane. After blocking the membranes with 5% non-fat milk for 2 h, the membranes were incubated with different primary antibodies at 4°C overnight, then incubated with secondary antibodies for 2 h. Each protein band was detected by enhanced chemiluminescence kits and quantified via Image J.

2.8. Immunofluorescence confocal

To determine NF-κB (p65) nuclear translocation, LPS was used to treat RAW264.7 cells with or without test compounds for 1 h. Cells were subsequently immobilized by paraformaldehyde containing 0.1% Triton, followed by incubation of p65 antibody at 4°C overnight. After incubating with Alexa Flour 568 conjugated-secondary antibody for 1 h, 4,6-diamidino-2-phenylindole (DAPI, Beyotime) was employed for cell dyeing for 15 min. For LPS/TLR4 complex assay, cells were incubated with the test compounds for 24 h, and co-incubated with LPS488 (10 μg/ml) for 12 h, then stained by DAPI. Subsequently, the immunofluorescence of p65 subunit translocation to nucleus and LPS intake to cell membranes were investigated via laser confocal microscope (CarlZeiss LSM 880, Jena, Germany) [26].

2.9. Molecular docking and molecular dynamics (MD) simulations

Molecular docking was performed by Autodock Vina (Scripps Research Institute, USA) to clarify the binding mechanism between TLR4/MD2 complex (Protein Data Bank ID: 3FXI) and GRo (CID: 11815492). The TLR4/MD2 complex removed of water molecules and bound ligands was prepared for molecular docking analysis. The agonist-binding domain of TLR4/MD2 was confirmed as the ligand binding site of TLR4/MD2 and AMBER03 force field was utilized to perform MD simulations. Simply, the initiation of simulated annealing minimization was set at 298K, with velocities scaled down by 0.9 every 10 steps. Following energy minimization, the temperature was adjusted to minimize the influence of temperature control. Finally, 100-ns molecular dynamics simulations

were conducted at a rate of 2 fs, and the coordinates of the complexes were saved every 10 ps.

2.10. Surface plasmon resonance imaging (SPRi)

Kx5 S instrument (Plexera, USA) was utilized to monitor the process to further detect the interaction between TLR4/MD2 complex protein and GRo. Shortly, a chip was assembled with a plastic flow cell for sample loading. The optical architecture and operation details of the PlexArray HT were described previously [27]. GRo samples were prepared with phosphate buffer saline at 50, 100, 200, 400 μM concentrations, and a 10-mM glycine-HCl buffer was used as regeneration buffer. A typical binding curve was obtained by GRo at 2 ml/s for 300 s association and then flowing running buffer for 300 s dissociation, followed by 200 s regeneration buffer at 3 ml/s. The binding data were collected and analyzed by the commercial SPRi analysis software (Plexera SPR Data Analysis Module, Plexera, USA).

2.11. Data analysis

Data were shown as mean ± standard deviation (SD) and were analyzed by one-way analysis of variance for comparisons between multiple groups using SPSS 21.0 (IBM Corporation, Armonk, NY, USA). A difference of $p < 0.05$ was considered significant statistically.

3. Results

3.1. P. ginseng inhibited LPS-induced lung injury and inflammation

To detect whether *P. ginseng* attenuated LPS-mediated lung damage *in vivo*, the pathological damages in lung tissue were measured by H&E staining. As indicated in Fig. 1A, LPS administration resulted in destructive alterations compared to the control group, including extensive alveolar wall thickening, infiltration of inflammatory cells, and interstitial edema. However, treatment with *P. ginseng* as well as DEX effectively inhibited lung pathological lesions. Moreover, the lung injury was evaluated semi-quantitatively based on histological examination, and the lung injury score was markedly decreased by *P. ginseng* and DEX (Fig. 1B). Interestingly, the effect of *P. ginseng* at a high dose was equivalent to the effect of DEX, as there was no significant difference between *P. ginseng*-treated (200 mg/kg) and DEX-treated groups. To further test the influence of *P. ginseng* on pro-inflammatory factors, TNF-α, IL-6, and IL-1β expression was detected. *In vivo*, we found the mRNA levels of TNF-α, IL-6 and IL-1β in lung tissue in the LPS group were increased in comparison to the control group. However, *P. ginseng* or DEX administration alleviated the LPS-induced over-expression of TNF-α, IL-6 and IL-1β mRNA levels (Fig. 1C—E). Similarly, the production of TNF-α, IL-6, and IL-1β in serum were reduced by *P. ginseng* as well as DEX as confirmed by ELISA assay (Fig. 1F—H). Notably, the effect of high dose of *P. ginseng* was not significant statistically compared to that of DEX on mRNA levels and production of TNF-α, IL-6, and IL-1β. Briefly, the effect of 200 mg/kg *P. ginseng* on LPS-induced lung injury was equivalent to that of DEX. Additionally, in the toxicity experiment, the serum AST levels of *P. ginseng* groups were not significant compared to that of control group and ALT levels were also similar between the groups, indicating that *P. ginseng* in 50-200 mg/kg dose is relatively safe for
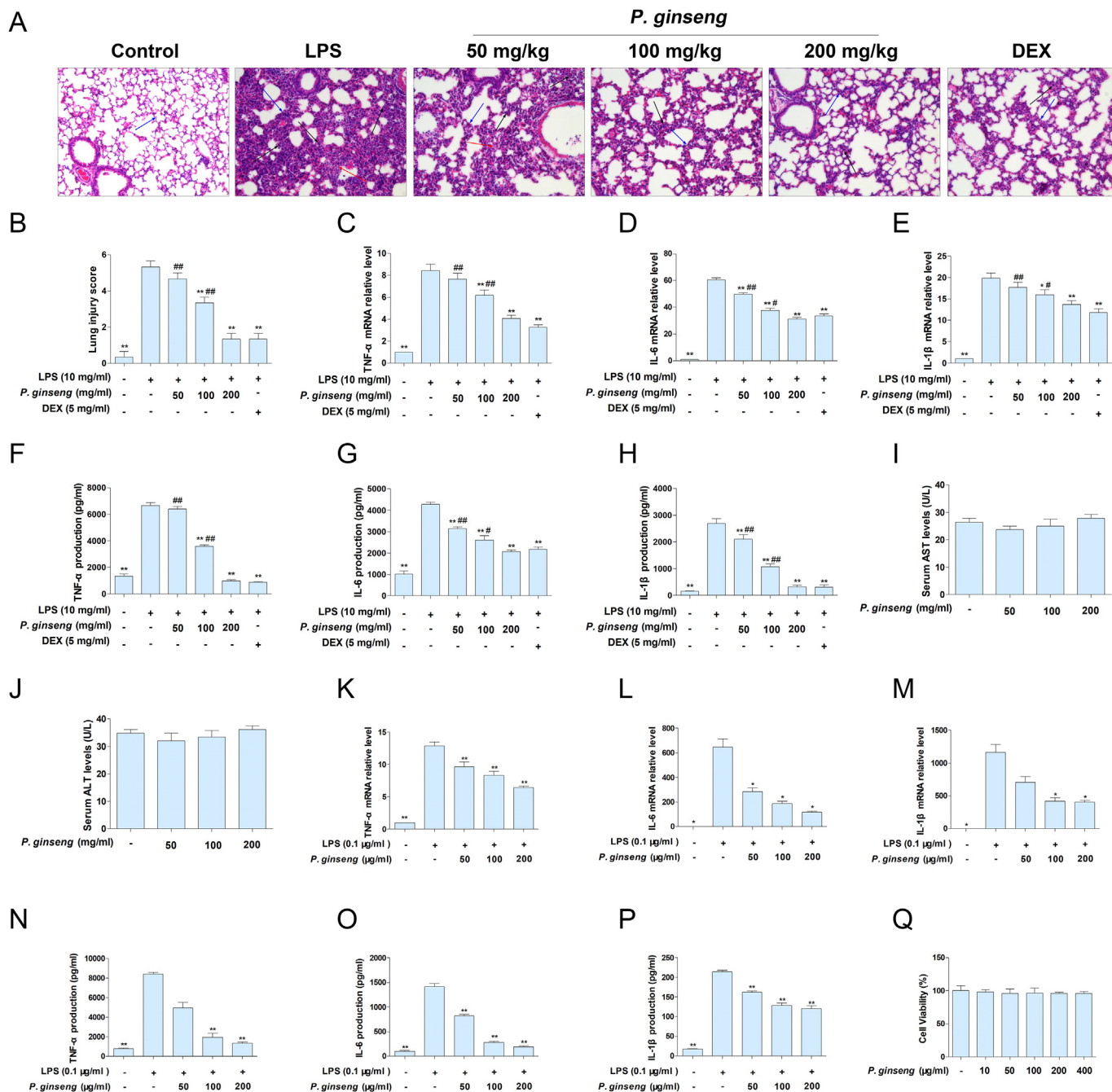
Fig. 1. *P. ginseng* suppressed LPS-triggered lung injury and inflammation. (A) The pathological images in lung tissue by H&E staining, the blue arrows indicate the alveolar wall, the black arrows represent infiltration of inflammatory cells, the red arrows indicate interstitial edema (magnification, 200 ×). (B) The lung injury score assessed semi-quantitatively according to the pathological examination. (C-E) Relative mRNA expression of TNF-α, IL-6, and IL-1β in lung tissue. (F–H) The production of TNF-α, IL-6, and IL-1β in serum tested by ELISA. (I) The serum AST levels of *P. ginseng*. (J) The serum ALT levels of *P. ginseng*. (K-M) Relative mRNA expression of TNF-α, IL-6 and IL-1β in RAW264.7 cells. (N–P) The production of TNF-α, IL-6 and IL-1β in cells supernatant. (Q) Cell viability with or without *P. ginseng* by MTT assay. Data were shown as mean ± SD (n = 4). *$p < 0.05$, **$p < 0.01$, vs the LPS group. #$p < 0.05$, ##$p < 0.01$, vs the LPS + DEX group. *P. ginseng*, *Panax ginseng* Meyer; LPS, lipopolysaccharide; TNF, tumor necrosis factor; IL, interleukin; H&E, haematoxylin and eosin; ELISA, enzyme-linked immunosorbent assay; SD, standard deviation.

using in murine model (Fig. 1I–J). *In vitro*, cells were incubated with *P. ginseng* (50, 100, and 200 μg/ml) for 24 h, then co-incubated with LPS (0.1 μg/ml) for 6 h. As shown in Fig. 1K-M, TNF-α, IL-6, and IL-1β mRNA levels were elevated after LPS stimulation. However, *P. ginseng* dose-dependently reduced gene expression of these pro-inflammatory factors. Consistently, the production of TNF-α, IL-6,

and IL-1β were remarkably lessened by *P. ginseng* in a dose-dependent manner (Fig. 1N–P). Additionally, MTT showed that *P. ginseng* had no toxicity toward RAW264.7 cells up to 400 μg/ml (Fig. 1Q). Our results suggested that *P. ginseng* suppressed pathological damages of lung tissue and expression of TNF-α, IL-6, and IL-1β induced by LPS *in vivo* and *in vitro*.
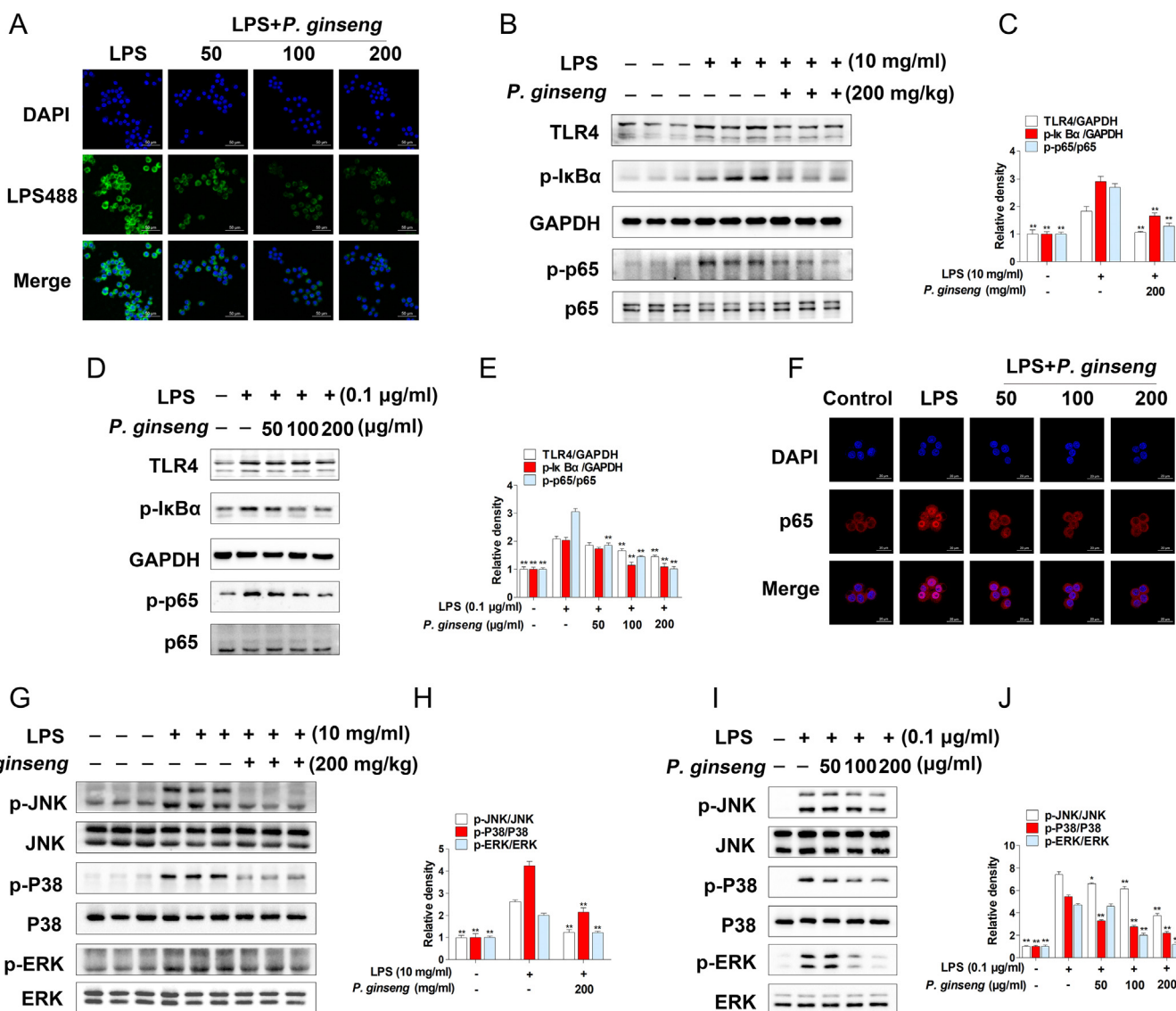
Fig. 2. *P. ginseng* suppressed NF-κB and MAPKs activation via blocking LPS binding to TLR4. (A) Effects of *P. ginseng* on the binding between fluorescence-labeled LPS (LPS488) and RAW264.7 cell membranes. Expression (B) and density analysis (C) of TLR4, phosphorylated IκBα and p65 in lung tissue. Expression (D) and density analysis (E) of TLR4, phosphorylated IκBα and p65 in RAW264.7 cells. (F) Effects of *P. ginseng* on NF-κB (p65) translocation from cytoplasm to nucleus. Expression (G) and density analysis (H) of phosphorylated JNK, P38 and ERK in lung tissue. Expression (I) and density analysis (J) of phosphorylated JNK, P38 and ERK in RAW264.7 cells. Data were shown as mean ± SD (n = 3). $*p < 0.05$, $**p < 0.01$, vs the LPS group. TLR4, Toll like receptor 4; NF-κB, nuclear factor-κB; MAPKs, mitogen-activated protein kinases; IκB, inhibitory κB; JNK, c-Jun N-terminal kinase; ERK, extracellular signal-regulated kinase.

3.2. P. ginseng inhibited NF-κB and MAPKs activation by blocking LPS binding to TLR4

The TLR4 signaling has an essential role in inflammation mediated by LPS. Herein, we detected whether *P. ginseng* suppressed the binding between LPS and TLR4. As shown in Fig. 2A, *P. ginseng* blocked LPS488 binding to cell membranes dose-dependently. Consistently, western blotting showed that *P. ginseng* significantly inhibited LPS-mediated over-expression of TLR4 in lung tissue (Fig. 2B–C). Additionally, *P. ginseng* dose-dependently reduced LPS-mediated over-expression of TLR4 in RAW264.7 cells (Fig. 2D–E). NF-κB and MAPKs are downstream elements of TLR4, which subsequently activate various inflammatory responses [28]. Since NF-κB activation results from phosphorylated IκBα, which is crucial for its degradation and p65 subunit nuclear translocation [29], we explored whether *P. ginseng*

affected IκB-α and p65 phosphorylation. We found that the phosphorylation levels of IκBα and p65 were increased under LPS treatment, which indicated that LPS activated NF-κB pathway. Oppositely, *P. ginseng* significantly inhibited the phosphorylation levels of IκBα and p65 *in vivo* (Fig. 2B–C). Consistent with TLR4 analysis, Fig. 2D–E revealed that the phosphorylation levels of IκBα and p65 *in vitro* were significantly inhibited by *P. ginseng*. Moreover, we further detected whether *P. ginseng* attenuated NF-κB (p65) subunit nuclear translocation. As revealed in Fig. 2F, LPS stimulation induced p65 nuclear translocation. However, *P. ginseng* dramatically inhibited p65 translocation from cytoplasm to nucleus. Moreover, we found that the phosphorylation levels of MAPKs (JNK, P38, ERK) were reduced obviously with treatment of *P. ginseng* without altering total levels of MAPKs *in vivo* (Fig. 2G–H). Similarly, *P. ginseng* pretreatment dose-dependently reduced the phosphorylation levels of MAPKs *in vitro* (Fig. 2I–J). Research

demonstrates that MAPK phosphorylates transcription factors such as c-Jun, c-Fos, and activating transcription factor 2 (ATF2), ultimately leading to the expression of inflammatory factors [30]. Therefore, we further explored whether *P. ginseng* inhibited the expression of c-Jun, c-Fos and ATF2. As shown in Supplementary Figs. S2A-B, *in vivo*, the phosphorylation levels of c-Jun, c-Fos and ATF2 were increased under LPS treatment, while *P. ginseng* management markedly suppressed the phosphorylation levels without changing the total proteins. Consistently, *in vitro*, the phosphorylation levels of c-Jun, c-Fos and ATF2 were inhibited by *P. ginseng* dose-dependently (Figs. S2C-D). The results firmly indicated that *P. ginseng* suppressed the activation of NF-κB and MAPKs signaling pathways via blocking LPS binding to TLR4.

3.3. GRo directly targeted TLR4

GRo, an oleanolic saponin of *P. ginseng*, has been revealed to inhibit IL-1β-triggered inflammation in rat chondrocytes via suppressing NF-κB [31]. In addition, GRo was discovered to inhibit LPS-induced cyclooxygenase-2 (COX-2) and inducible nitric oxide synthase (iNOS) in RAW264.7 cells [32]. We hypothesized that GRo might be an active component of the anti-inflammatory roles of *P. ginseng.* However, it remains unclear whether GRo prevents inflammation via inhibition of TLR4. Molecular docking and MD simulations were subsequently utilized to evaluate the interaction between TLR4/MD2 complex and GRo. The three-dimensional conformations of TLR4-MD2-LPS complex and TLR4-MD2-GRo complex were displayed in Fig. 3A and B, respectively. The binding energy between TLR4/MD2 and GRo was −9.285 kcal/mol. Additionally, the surface visualization models of TLR4-MD2-GRo complex at 0ns and 100ns were displayed in Fig. 3C. GRo tightly bound to TLR4/MD2 binding site center during the whole process of MD simulation. Moreover, as displayed in Fig. 3D, the progression of the root mean square deviation (RMSD) of all atoms was from 0 ns to 100 ns, of which the RMSD of MD2-GRo bound part was stable at about 2-3 Å. For further clarification of the integration mechanism of TLR4-MD2-GRo complex, immunofluorescence and SPRi were performed. As shown in Fig. 3E, LPS immunofluorescence demonstrated that LPS488 binding to cell membranes was dose-dependently suppressed by GRo. SPRi revealed that GRo rapidly bound to TLR4/MD2 complex recombinant protein with an equilibrium dissociation constant (K_D) value of 1.16×10^{-9} M, suggesting an excellent binding affinity (Fig. 3F). The outcomes robustly implicated that GRo directly targeted TLR4.

3.4. GRo inhibited LPS-induced inflammation

To explore whether GRo exerted anti-inflammatory effects, *in vitro* as well as *in vivo* assays were performed. MTT displayed that cell viability in GRo groups (10-400 μM) was similar with the control group, implicating that GRo was not toxic on RAW264.7 cells (Fig. 4A). The mRNA expression of TNF-α, IL-6, and IL-1β enhanced when LPS was used, but dose-dependently decreased under GRo treatment (Fig. 4B−D). From ELISA experiments, GRo remarkably lessened the production of TNF-α, IL-6, and IL-1β at concentrations from 50 μM to 200 μM (Fig. 4E−G). Further animal experiments demonstrated that LPS administration exhibited the infiltration of inflammatory cells, alveolar wall thickening, and interstitial edema as confirmed by H&E staining. However, GRo or DEX administration significantly attenuated the lung pathological lesions and the lung injury score, which the effect of 80 mg/kg GRo

was similar to that of DEX (Fig. 4H−I). Moreover, as Fig. 4J-O shown, either mRNA expression or pro-inflammatory cytokines secretion was decreased by GRo treatment in mice. Additionally, DEX also drastically abated the expression of TNF-α, IL-6, and IL-1β on mRNA and secretion levels. Interestingly, GRo at a high dose (80 mg/kg) exerted a remarkable activity in suppression IL-6 expression compared to that of DEX. However, there was no significant difference on the expression of TNF-α and IL-1β between 80 mg/kg GRo-treated and DEX-treated groups. Animal toxicity experiment displayed that the serum AST and ALT levels in GRo groups (20-80 mg/kg) were similar with the control group, implicating that GRo in 20-80 mg/kg dose is nontoxic and secure for using in murine model (Fig. 4P-Q).

3.5. GRo inhibited TLR4-induced the activation of NF-κB and MAPKs signaling pathways

To explore whether GRo inhibited the expression of TLR4 and its signal downstream, the actions of TLR4/NF-κB/MAPKs signaling pathways were tested. As Fig. 5A−B shown, *in vivo*, administration with GRo significantly suppressed TLR4 expression, IκBα and p65 phosphorylation, all of which were increased by LPS treatment. Similarly, the phosphorylation levels of MAPKs in lung tissue were notably decreased by GRo (Fig. 5C−D). We further explored the effects of GRo *in vitro*. Briefly, cells were incubated with GRo for 24 h, then co-incubated with LPS for 1 h. Western blotting showed that the TLR4 expression and phosphorylation of IκBα, p65 enhanced in LPS group while were decreased by GRo dose-dependently (Fig. 5E−F). And GRo significantly suppressed the phosphorylation levels of JNK, P38, and ERK without altering the total proteins (Fig. 5G−J). Moreover, GRo effectively attenuated the nuclear translocation of p65 subunit (Fig. 5K). Additionally, we further investigated the effect of GRo on the expression of p65 in cytoplasm and nucleus. As shown in Supplementary Fig. S1, LPS increased the p65 nucleus accumulation. However, GRo significantly decreased p65 nucleus accumulation and increased the cytoplasmic expression of p65. Moreover, the phosphorylation levels of c-Jun, c-Fos and ATF2 were inhibited by GRo without change of the total proteins *in vivo* and *in vitro* (Figs. S2E-H). The results implicated that GRo suppressed TLR4-induced the activation of NF-κB and MAPKs signaling pathways.

3.6. Inhibition of TLR4 signaling pathway did not enhance the inhibitory effect of GRo in RAW264.7

To confirm whether the inhibitory role of GRo in RAW264.7 was due to the inhibition of TLR4 signaling, TLR4 was blocked using TAK242, a selective TLR4 inhibitor, followed by detection of cell viability, mRNA levels of TNF-α, IL-6 and IL-1β and expression of relevant proteins of RAW264.7 cells. As displayed in Fig. 6A, treatment with TAK242 exerted no cell toxicity as compared with the control group. qRT-PCR demonstrated that mRNA levels of TNF-α, IL-6 and IL-1β were significantly suppressed by GRo and TAK242 pretreatment. Nevertheless, the suppressive impact of co-treatment of GRo and TAK242 failed to further significantly inhibit the pro-inflammatory factors in comparison to the treatment of GRo or TAK242 alone (Fig. 6B−D). Consistently, TLR4 expression and phosphorylation levels of IκBα, p65 as well as MAPKs of GRo and TAK242 co-treatment group were not significantly further attenuated in comparison with cells incubated with TAK242 alone (Fig. 6E−F). The outcomes implicated that the
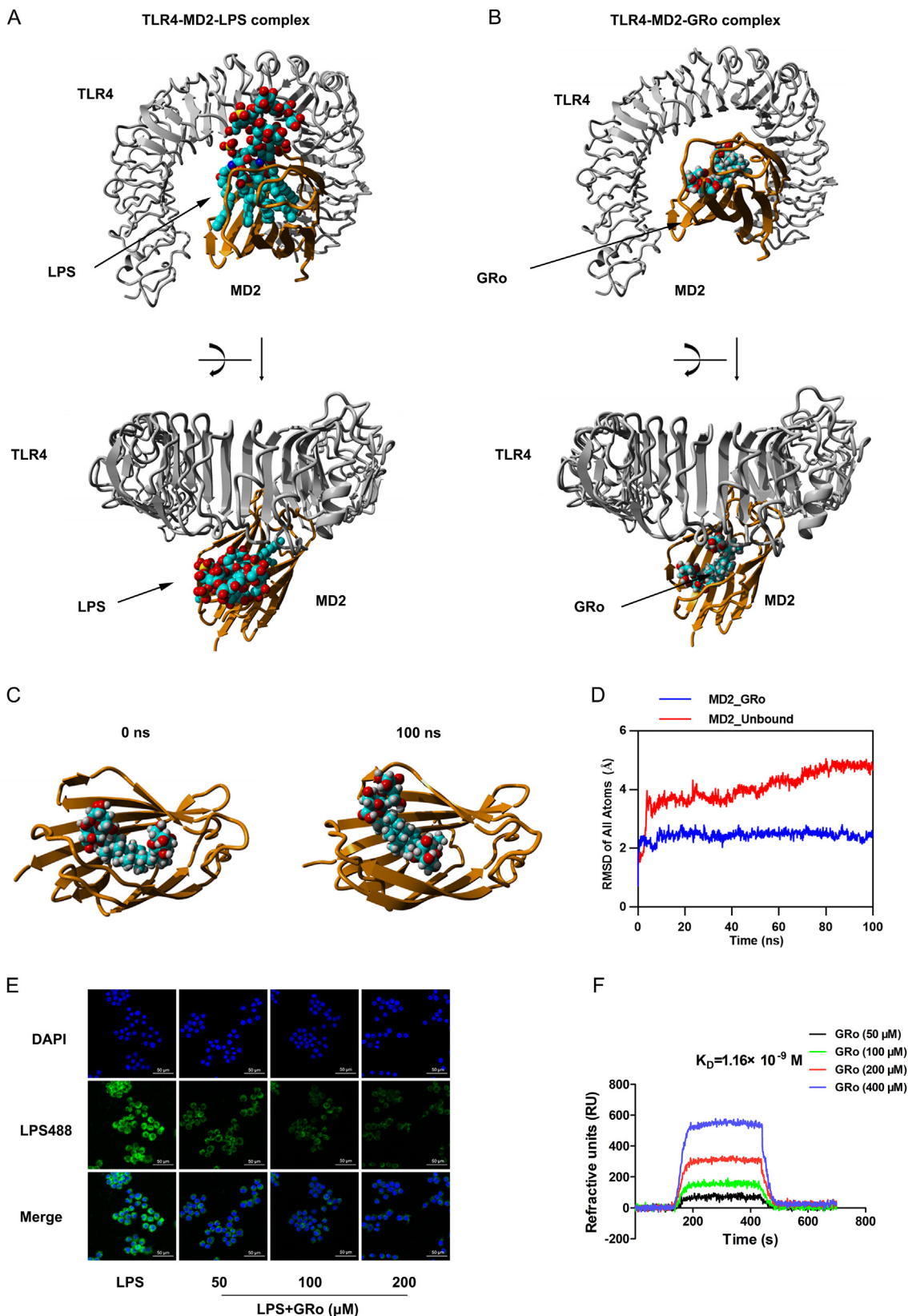
Fig. 3. GRo inhibited TLR4 directly. (A) Three-dimensional crystal structure of TLR4-MD2-LPS complex. (B) Three-dimensional crystal structure of TLR4-MD2-GRo complex. (C) Surface presentation of TLR4-MD2-GRo complex in 0ns and 100ns. (D) Root mean square deviation (RMSD) of heavy atoms of TLR4-MD2-GRo complexes (blue) and unbound TLR4-MD2-LPS (red). (E) Effects of GRo on fluorescence-labeled LPS (LPS488) binding to cell membranes. (F) The SPRi fitting curves of GRo (50, 100, 200, and 400 μM) binding to TLR4/MD2 complex protein. GRo, ginsenoside Ro; MD2, myeloid differentiation factor 2; SPRi, Surface Plasmon Resonance imaging; RU, refractive units.
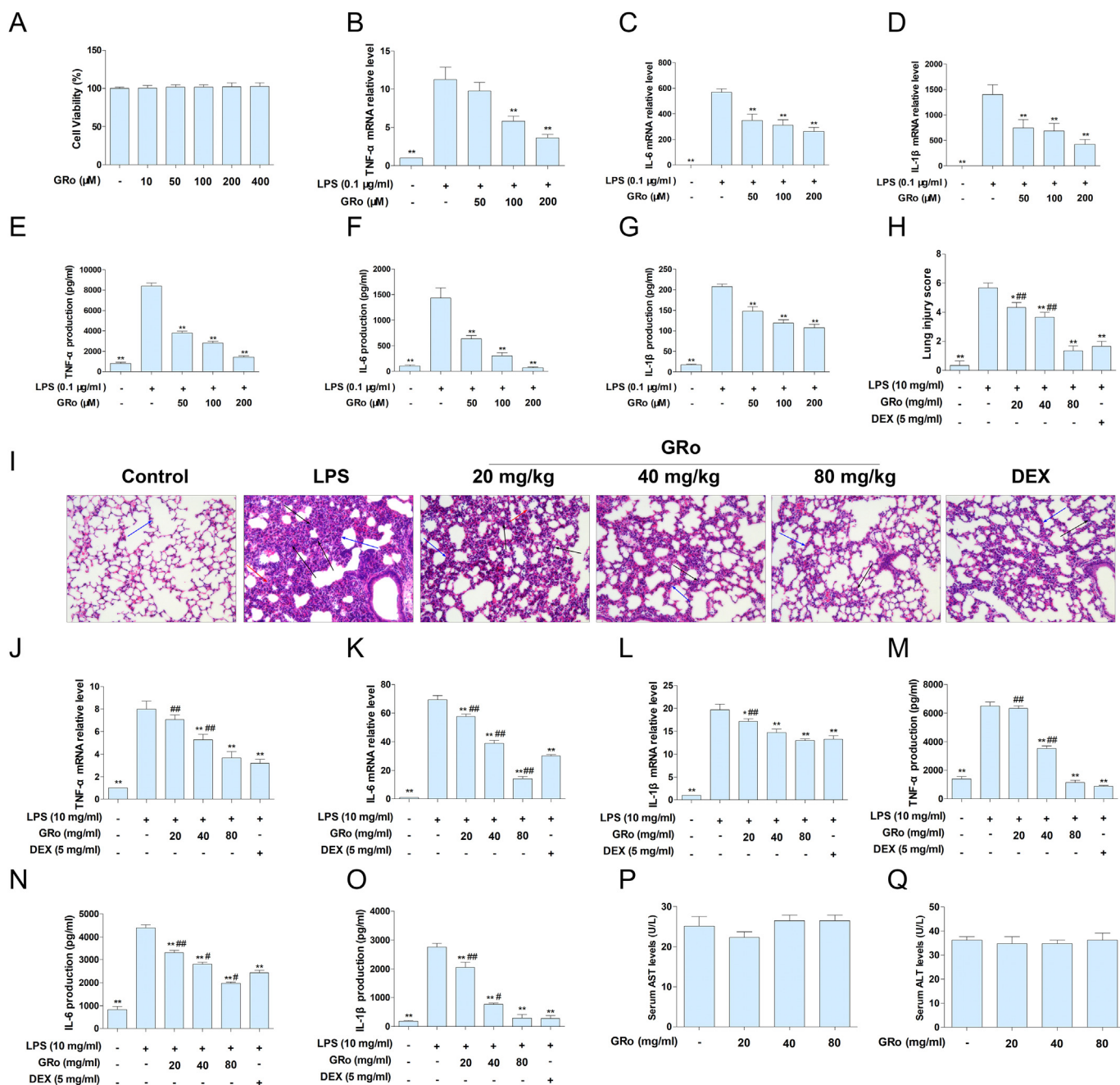
Fig. 4. GRo suppressed LPS-induced inflammation *in vivo* and *in vitro*. (A) Cell viability with or without GRo via MTT assay. (B-D) Relative mRNA expression of TNF-α, IL-6, and IL-1β *in vitro*. (E-G) The production of TNF-α, IL-6, and IL-1β in cells supernatant. (H) The lung injury score was assessed semi-quantitatively. (I) The pathological images in lung tissue by H&E staining, the blue arrows indicate the alveolar wall, the black arrows represent infiltration of inflammatory cells, the red arrows indicate interstitial edema (magnification, 200 ×). (J-L) Relative mRNA expression of TNF-α, IL-6 and IL-1β in lung tissue. (M-O) TNF-α, IL-6, and IL-1β production in serum. Data were shown as mean ± SD (n = 4). *$p < 0.05$, **$p < 0.01$, vs the LPS group. #$p < 0.05$, ##$p < 0.01$, vs the LPS + DEX group. GRo, ginsenoside Ro; LPS, lipopolysaccharide.

suppression of TLR4 signaling pathway did not strengthen the inhibitory effect of GRo in RAW264.7 cells. Therefore, the anti-inflammatory ability of GRo was due to the inhibition of TLR4 signaling pathway.

4. Discussion

Inflammation is vitally involved in the pathogenesis of ALI, and pro-inflammatory cytokines are key determinants to aggravate the extent of inflammation. Therefore, inhibition of pro-inflammatory cytokines contributes to attenuated inflammation, which is the therapeutic basis for inflammation-related diseases. *P. ginseng* has been found to protect against inflammatory diseases. For example, Park SB illustrates that wood-cultivated ginseng suppressed IL-1β, TNF-α and inflammatory enzymes like iNOS and COX-2 expression [33]. In this research, we reveals the inhibitory influence of *P. ginseng* on pro-inflammatory cytokines secretion through down-regulating the mRNA levels. Notably, we found that the effect of high dose of *P. ginseng* on LPS-induced lung injury was equivalent to that of DEX. Our present findings will enrich the current understanding of *P. ginseng* on expression of inflammatory factors.
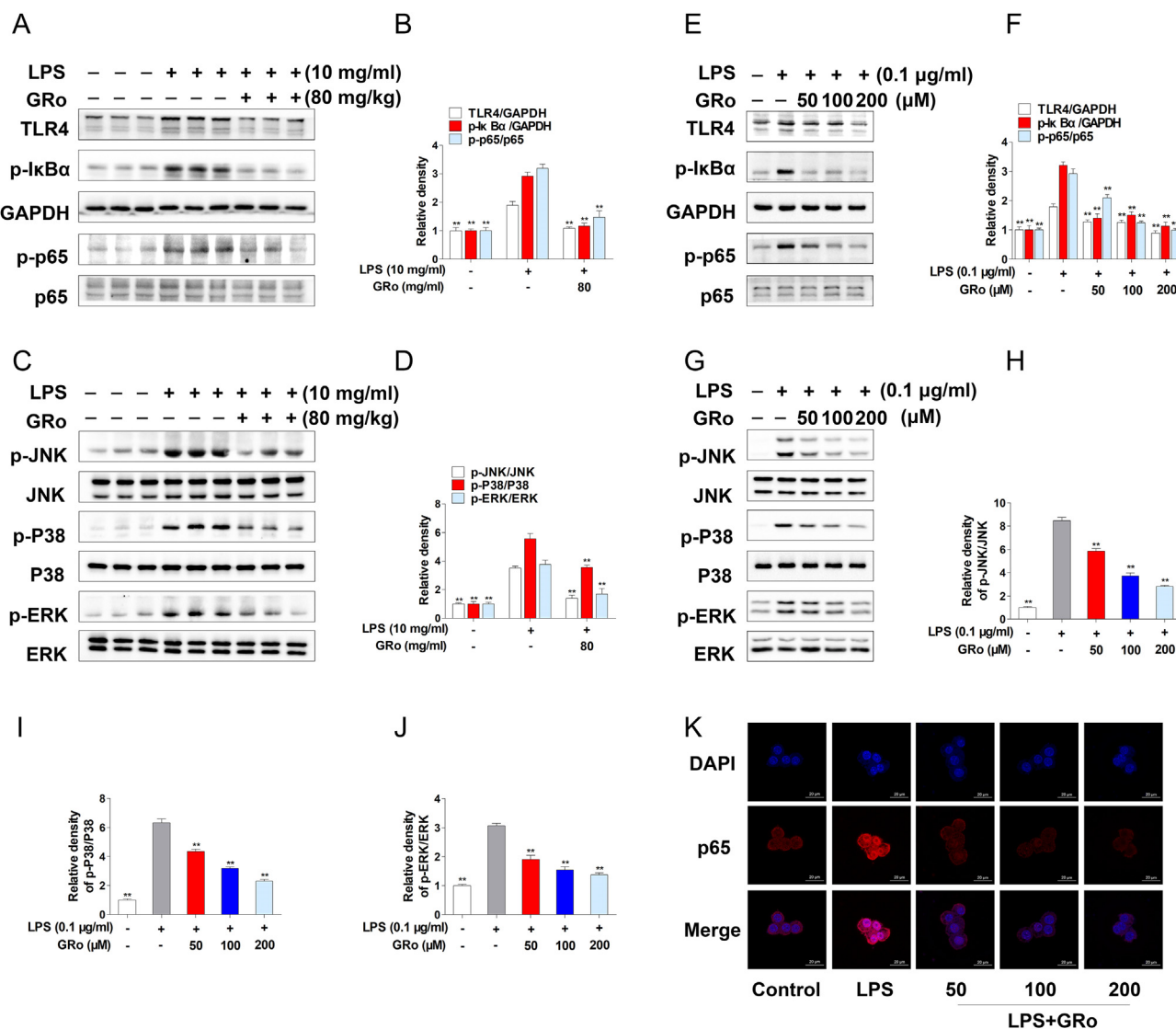
Fig. 5. GRo inhibited TLR4-induced the activation of NF-κB and MAPKs signaling *in vivo* and *in vitro*. Expression (A) and density analysis (B) of TLR4, phosphorylated IκBα and p65 in lung tissue. Expression (C) and density analysis (D) of phosphorylated JNK, P38 and ERK in lung tissue. Expression (E) and density analysis (F) of TLR4, phosphorylated IκBα and p65 in RAW264.7 cells. Expression (G) and respective density analysis (H-J) of phosphorylated JNK, P38 and ERK in RAW264.7 cells. (K) The immunofluorescence of NF-κB (p65) translocation to nucleus. Data were shown as mean ± SD (n = 3). *$p < 0.05$, **$p < 0.01$, vs the LPS group. GRo, ginsenoside Ro; TLR4, Toll like receptor 4; NF-κB, nuclear factor- κB; MAPKs, mitogen-activated protein kinases.

However, the active compounds and the underlying mechanism of *P. ginseng* are not explored thoroughly.

Toll-like receptors have an essential effect in external pathogen infections. Of note, TLR4 is a specific pattern recognition receptor for LPS stimulation, thereby triggering inflammatory responses [34]. Therefore, inactive TLR4 signaling pathway is of great significance. Intriguingly, we found that *P. ginseng* significantly suppressed TLR4 expression and LPS binding to cell membranes dose-dependently, suggesting that *P. ginseng* inhibited LPS/TLR4 interaction. Generally, TLR4/MD2 heterodimer specifically triggers intracellular signaling pathways activation such as NF-κB and MAPKs, subsequently causing inflammatory factors release, even cell death [35]. NF-κB exists in the cytoplasm and is inactivated by combining with IκB under normal condition, of which IκB-α is the most important [36]. Phosphorylation of IκBα can cause subsequent ubiquitination and proteasome degradation, thereby promoting p65 subunit nuclear translocation and inducing the expression of inflammatory cytokines [29,37]. Therefore, we further investigated

whether *P. ginseng* inhibited NF-κB activation, we found that *P. ginseng* inhibited the phosphorylation levels of IκB-α and p65 *in vivo* and *in vitro*. Consistently, *P. ginseng* also suppressed p65 translocation to nucleus. Additionally, MAPKs can phosphorylate c-Jun, c-Fos, and ATF2, ultimately generate excessive inflammatory factors, playing a crucial role in pathogenesis of inflammation [38,39]. Consequently, we further found that *P. ginseng* decreased MAPKs, c-Jun, c-Fos, and ATF2 phosphorylation levels without altering total proteins. Our results are consistent to previous research showing that ginseng could suppress the activation of NF-κB and MAPK [33].

Molecular docking as an effective predicting tool enables the recognition of new compounds at a molecular level for drug discovery based on computer structure simulation, exploring the protein-ligand interaction [40]. In addition, as a forefront of optical sensing and high-throughput detection technology, SPRi explores the multi-molecular interactions label-freely in a real time [41,42]. Hence, molecular docking, SPRi and immunofluorescence were
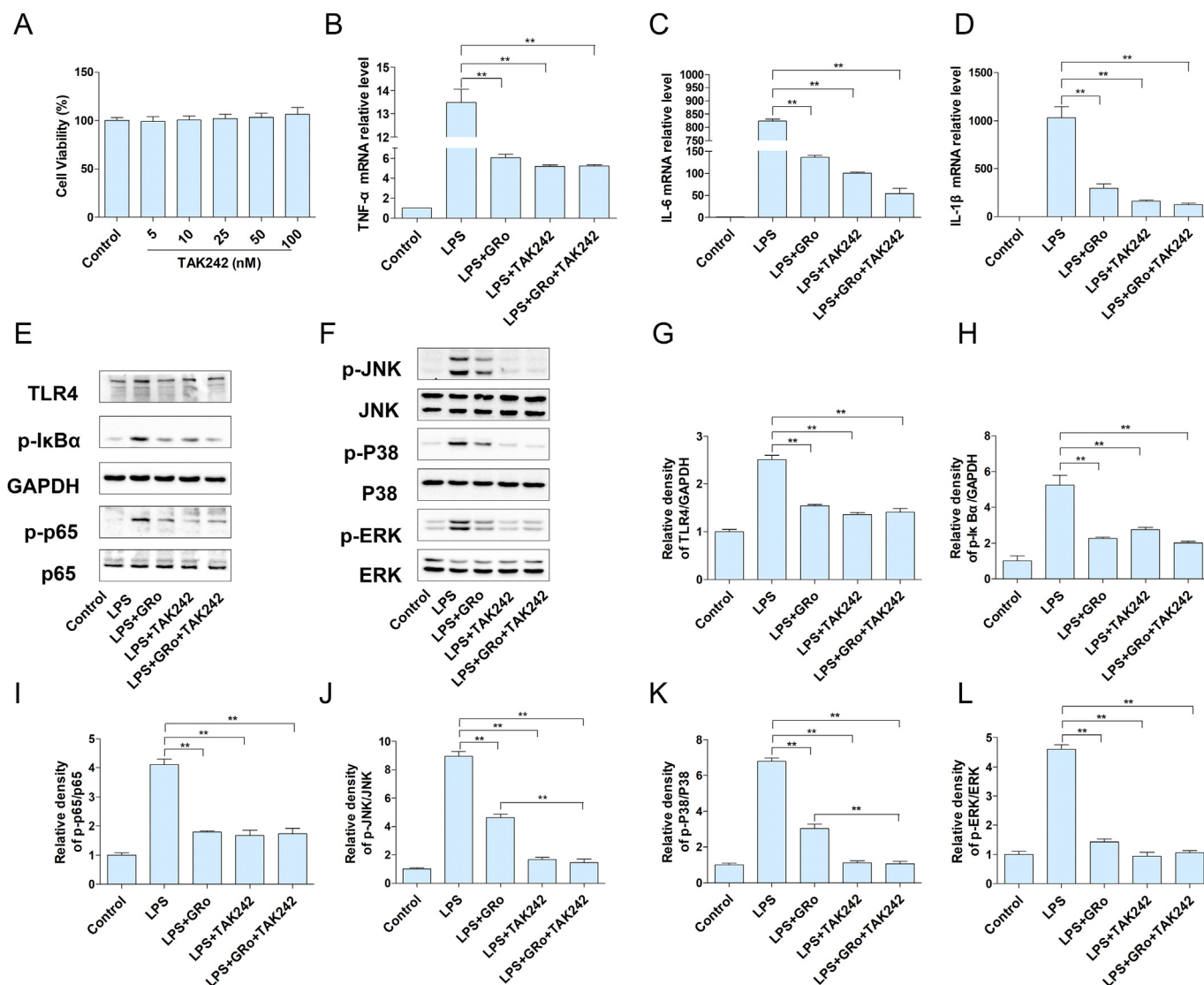
Fig. 6. Inhibition of TLR4 signaling pathway did not increase the inhibitory effect of GRo in RAW264.7 cells. TAK242 was applied to block TLR4 signaling pathway. RAW264.7 cells were incubated with 10 nM TAK242 for 1 h, 200 μM GRo for another 24 h and co-incubated with LPS. (A) Cell viability under treatment with TAK242. (B-D) Relative mRNA expression of TNF-α, IL-6, and IL-1β. Expression (E) and respective density analysis (G-I) of TLR4, phosphorylated IκBα, and p65. Expression (F) and respective density analysis (J-L) of phosphorylated JNK, P38, and ERK. Data were shown as mean ± SD (n = 3). *$p < 0.05$, **$p < 0.01$. TLR4, Toll like receptor 4; TAK242, resatorvid.

performed to further explore the active ingredient of *P. ginseng* as the TLR4 inhibitor. In the present study, the binding energy of TLR4-MD2-GRo complex suggested robust binding. Additionally, MD simulation indicated that GRo steadily bound to the center of active pocket of TLR4/MD2 complex, and SPRi revealed that the K_D value was 1.16×10^{-9} M, indicating an excellent binding affinity. Immunofluorescence showed that treatment with GRo inhibited LPS488 binding to the membranes of RAW264.7 macrophages dose-dependently. Therefore, GRo was identified as a direct TLR4 inhibitor. Moreover, GRo not only relieved the LPS-induced pathological damages of lung tissue, but also suppressed the transcription and secretion of TNF-α, IL-6 and IL-1β. Interestingly, *in vivo*, GRo at a high dose was superior to DEX in decreasing IL-6 expression. Additionally, GRo blocked TLR4 expression and phosphorylation levels of MAPKs and NF-κB. Afterwards, to further explore whether the suppressive impact of GRo in RAW264.7 cells was caused by TLR4 signaling suppression, TAK242, a specific TLR4 inhibitor, was utilized for further assays. Consequently, the inhibitory effect of GRo and TAK242 co-treatment on pro-inflammatory

cytokines was not significantly enhanced in comparison with the treatment with GRo or TAK242 alone. The anti-inflammatory impact of GRo was equivalent to that of TAK242. Collectively, the above outcomes suggested that TLR4 was the major pharmacological target of GRo.

5. Conclusion

Summarily, our results reveal that GRo exerts anti-inflammatory effect by directly inhibiting TLR4 signaling pathways. GRo may serve as a natural therapeutic compound for inflammation-associated disorders.

Acknowledgments

2019A1515110367), Traditional Chinese Medicine Bureau of Guangdong Province (Nos. 20173016, 20201392), Project of Huizhou science and Technology Bureau (No. 2016C0408023).

Appendix A. Supplementary data

Supplementary data to this article can be found online at https://doi.org/10.1016/j.jgr.2021.05.011.

References

[1] Takeuchi O, Akira S. Pattern recognition receptors and inflammation. Cell 2010;140(6):805–20.
[2] Xiao TS. Innate immunity and inflammation. Cell Mol Immunol 2017;14(1):1–3.
[3] Yun M, Yi Y. Regulatory roles of ginseng on inflammatory caspases, executioners of inflammasome activation. J Ginseng Res 2020;44(3):373–85.
[4] Ayaz F. Heteroleptic ruthenium polypyridyl complex had differential effects on the production of pro-inflammatory cytokines TNFα, IL1β, and IL6 by the mammalian macrophages in vitro. Inflammation 2019;42(4):1383–8.
[5] Yi Y. Ameliorative effects of ginseng and ginsenosides on rheumatic diseases. J Ginseng Res 2019;43(3):335–41.
[6] Hansson GK. Inflammation, atherosclerosis, and coronary artery disease. N Engl J Med 2005;352(16):1685–95.
[7] Vasefi M, Hudson M, Ghaboolian-Zare E. Diet associated with inflammation and alzheimer's disease. J Alzheimers Dis Rep 2019;3(1):299–309.
[8] Rorato R, Borges BC, Uchoa ET, Antunes-Rodrigues J, Elias CF, Elias L. LPS-induced low-grade inflammation increases hypothalamic JNK expression and causes central insulin resistance irrespective of body weight changes. Int J Mol Sci 2017;18(7):1431.
[9] Schottenfeld D, Beebe-Dimmer J. Chronic inflammation: a common and important factor in the pathogenesis of neoplasia. CA Cancer J Clin 2006;56(2):69–83.
[10] Rubenfeld GD, Caldwell E, Peabody E, Weaver J, Martin DP, Neff M, Stern EJ, Hudson LD. Incidence and outcomes of acute lung injury. N Engl J Med 2005;353(16):1685–93.
[11] Zhao J, Yu H, Liu Y, Gibson SA, Yan Z, Xu X, Gaggar A, Li P, Li C, Wei S, et al. Protective effect of suppressing STAT3 activity in LPS-induced acute lung injury. American Journal of Physiology. Am J Physiol Lung Cell Mol Physiol 2016;311(5):L868–80.
[12] Ware LB, Matthay MA. The acute respiratory distress syndrome. N Engl J Med 2000;342(18):1334–49.
[13] Bekeredjian-Ding I, Jego G. Toll-like receptors-sentries in the B-cell response. Immunology 2009;128(3):311–23.
[14] Ryu JK, Kim SJ, Rah SH, Kang JI, Jung HE, Lee D, Lee HK, Lee JO, Park BS, Yoon TY, et al. Reconstruction of LPS transfer cascade reveals structural determinants within LBP, CD14, and TLR4-MD2 for efficient LPS recognition and transfer. Immunity 2017;46(1):38–50.
[15] Płóciennikowska A, Hromada-Judycka A, Borzęcka K, Kwiatkowska K. Co-operation of TLR4 and raft proteins in LPS-induced pro-inflammatory signaling. Cell Mol Life Sci 2015;72(3):557–81.
[16] Billod JM, Lacetera A, Guzmán-Caldentey J, Martín-Santamaría S. Computational approaches to toll-like receptor 4 modulation. Molecules 2016;21(8):994.
[17] Iqbal H, Rhee D. Ginseng alleviates microbial infections of the respiratory tract: a review. J Ginseng Res 2020;44(2):194–204.
[18] Wang C, Anderson S, Du W, He T, Yuan C. Red ginseng and cancer treatment. Chin J Nat Med 2016;14(1):7–16.
[19] Kim J. Pharmacological and medical applications of Panax ginseng and ginsenosides: a review for use in cardiovascular diseases. J Ginseng Res 2018;42(3):264–9.
[20] Yi Y. Ameliorative effects of ginseng and ginsenosides on rheumatic diseases. J Ginseng Res 2019;43(3):335–41.
[21] Lee JH, Min DS, Lee CW, Song KH, Kim YS, Kim HP. Ginsenosides from Korean Red Ginseng ameliorate lung inflammatory responses: inhibition of the MAPKs/NF-κB/c-Fos pathways. J Ginseng Res 2018;42(4):476–84.
[22] Zhu W, Cao FS, Feng J, Chen HW, Wan JR, Lu Q, Wang J. NLRP3 inflammasome activation contributes to long-term behavioral alterations in mice injected with lipopolysaccharide. Neuroscience 2017;343:77–84.
[23] Wu YT, Chen L, Tan ZB, Fan HJ, Xie LP, Zhang WT, Chen HM, Li J, Liu B, Zhou YC. Luteolin inhibits vascular smooth muscle cell proliferation and migration by inhibiting TGFBR1 signaling. Front Pharmacol 2018;9:1059.
[24] Gao H, Xiao D, Gao L, Li X. MicroRNA-93 contributes to the suppression of lung inflammatory responses in LPS-induced acute lung injury in mice via the TLR4/MyD88/NF-κB signaling pathway. Int J Mol Med 2020;46(2):561–70.
[25] Chen L, Su ZZ, Huang L, Xia FN, Qi H, Xie LJ, Xiao S, Chen QF. The AMP-activated protein kinase KIN10 is involved in the regulation of autophagy in arabidopsis. Front Plant Sci 2017;8:1201.
[26] Fan HJ, Zhao XS, Tan ZB, Liu B, Xu HL, Wu YT, Xie LP, Bi YM, Lai YG, Liang HF, et al. Effects and mechanism of action of Huang-Lian-Jie-Du-Tang in atopic dermatitis-like skin dysfunction in vivo and in vitro. J Ethnopharmacol 2019;240:111937.
[27] Wang Y, Wang C, Cheng Z, Zhang D, Li S, Song L, Zhou W, Yang M, Wang Z, Zheng Z, et al. SPRi determination of inter-peptide interaction by using 3D supramolecular co-assembly polyrotaxane film. Biosens Bioelectron 2015;66:338–44.
[28] Li MY, Sun L, Niu XT, Chen XM, Tian JX, Kong YD, Wang GQ. Astaxanthin protects lipopolysaccharide-induced inflammatory response in Channa argus through inhibiting NF-κB and MAPKs signaling pathways. Fish Shellfish Immunol 2019;86:280–6.
[29] Zandi E, Rothwarf DM, Delhase M, Hayakawa M, Karin M. The IkappaB kinase complex (IKK) contains two kinase subunits, IKKalpha and IKKbeta, necessary for IkappaB phosphorylation and NF-kappaB activation. Cell 1997;91(2):243–52.
[30] Cargnello M, Roux PP. Activation and function of the MAPKs and their substrates, the MAPK-activated protein kinases. Microbiol Mol Biol Rev 2011;75(1):50–83.
[31] Zhang XH, Xu XX, Xu T. Ginsenoside Ro suppresses interleukin-1β-induced apoptosis and inflammation in rat chondrocytes by inhibiting NF-κB. Chin J Nat Med 2015;13(4):283–9.
[32] Kim S, Oh MH, Kim BS, Kim WI, Cho HS, Park BY, Park C, Shin GW, Kwon J. Upregulation of heme oxygenase-1 by ginsenoside Ro attenuates lipopolysaccharide-induced inflammation in macrophage cells. J Ginseng Res 2015;39(4):365–70.
[33] Park SB, Park GH, Um Y, Kim HN, Song HM, Kim N, Kim H, Jeong JB. Wood-cultivated ginseng exerts anti-inflammatory effect in LPS-stimulated RAW264.7 cells. Int J Biol Macromol 2018;116:327–34.
[34] Plociennikowska A, Hromada-Judycka A, Borzecka K, Kwiatkowska K. Co-operation of TLR4 and raft proteins in LPS-induced pro-inflammatory signaling. Cell Mol Life Sci 2015;72(3):557–81.
[35] Li MY, Sun L, Niu XT, Chen XM, Tian JX, Kong YD, Wang GQ. Astaxanthin protects lipopolysaccharide-induced inflammatory response in Channa argus through inhibiting NF-κB and MAPKs signaling pathways. Fish Shellfish Immunol 2019;86:280–6.
[36] Brasier AR. The NF-kappaB regulatory network. Cardiovasc Toxicol 2006;6(2):111–30.
[37] Gilmore TD. Introduction to NF-kappaB: players, pathways, perspectives. Oncogene 2006;25(51):6680–4.
[38] Li S, Jang H, Zhang J, Nussinov R. Raf-1 cysteine-rich domain increases the affinity of K-Ras/Raf at the membrane, promoting MAPK signaling. Structure 2018;26(3):513–25.
[39] Liu HM, Lee TY, Liao JF. GW4064 attenuates lipopolysaccharide-induced hepatic inflammation and apoptosis through inhibition of the Toll-like receptor 4-mediated p38 mitogen-activated protein kinase signaling pathway in mice. Int J Mol Med 2018;41(3):1455–62.
[40] Pinzi L, Rastelli G. Molecular docking: shifting paradigms in drug discovery. Int J Mol Sci 2019;20(18):4331.
[41] Zhao S, Yang M, Zhou W, Zhang B, Cheng Z, Huang J, Zhang M, Wang Z, Wang R, Chen Z, et al. Kinetic and high-throughput profiling of epigenetic interactions by 3D-carbene chip-based surface plasmon resonance imaging technology. Proc Natl Acad Sci USA 2017;114(35):E7245–54.
[42] Scarano S, Scuffi C, Mascini M, Minunni M. Surface plasmon resonance imaging (SPRi)-based sensing: a new approach in signal sampling and management. Biosens Bioelectron 2010;26(4):1380–5.